

GANDALF: Gated Adaptive Network for Deep Automated Learning of Features

Manu Joseph¹,
Harsh Raj²,

¹Walmart Global Tech, Bangalore, KA, India

manu.joseph@walmart.com

²Dept. of Engineering Physics, Delhi Technological University, Delhi, India

Abstract

We propose a novel high-performance, interpretable, and parameter & computationally efficient deep learning architecture for tabular data, Gated Adaptive Network for Deep Automated Learning of Features (GANDALF). GANDALF relies on a new tabular processing unit with a gating mechanism and in-built feature selection called Gated Feature Learning Unit (GFLU) as a feature representation learning unit. We demonstrate that GANDALF outperforms or stays at-par with SOTA approaches like XGBoost, SAINT, FT-Transformers, etc. by experiments on multiple established public benchmarks. We have made available the code at https://github.com/manujosephv/pytorch_tabular under MIT License.

Introduction

Deep Learning(Goodfellow, Bengio, and Courville 2016) has revolutionized the field of machine learning, surpassing state-of-the-art systems in various domains such as computer vision (Krizhevsky, Sutskever, and Hinton 2017), natural language processing (Devlin et al. 2019), reinforcement learning(Silver et al. 2016). However, it has not made significant strides in tabular data analysis where state-of-the-art techniques typically rely on *shallow* models such as gradient boosted decision trees (GBDT)(Friedman 2001; Chen and Guestrin 2016; Ke et al. 2017; Prokhorenkova et al. 2018).

Recognizing the importance of deep learning in this context, several new architectures have been proposed(Arik and Pfister 2021; Popov, Morozov, and Babenko 2020) and a PyTorch-based deep learning library has been developed (PyTorch Tabular (Joseph 2021)).

Surveys conducted by Shwartz-Ziv and Armon (2022) and Borisov et al. (2021) highlight the existing gap between deep learning models and the GBDT state-of-the-art in terms of performance, training, and inference times. This discrepancy is further substantiated by the prevalence of shallow GBDT models in Kaggle competitions.

In this paper, our aim is to narrow this gap by proposing novel approaches and techniques. We introduce *Gated Adaptive Network for Deep Automated Learning of Features (GANDALF)*, a new deep learning architecture for tabular data.

Copyright © 2024, Association for the Advancement of Artificial Intelligence (www.aaai.org). All rights reserved.

In the following sections we will explain the design choices which make GANDALF a competitive model choice for tabular data. Through a large number of experiments on public benchmarks, we compare the proposed approach to leading GBDT implementations and other deep learning models and show that our model is accurate, parameter efficient, fast, and robust with lesser number of hyper parameters to tune.

Overall, our main contributions can be summarized as follows:

1. A new tabular data processing unit, the Gated Feature Learning Unit (GFLU), which can be used in place of regular FeedForward Blocks. The GFLU has feature selection and interpretability built into its design, making it a more powerful and flexible tool for tabular data analysis.
2. A new gating mechanism, inspired by Gated Recurrent Units (Cho et al. 2014), for representation learning. This mechanism allows the GFLU to learn more complex and informative representations of tabular data, which leads to improved performance on downstream tasks. To the best of our knowledge, this is the first time such an approach has been used to process non-temporal tabular data.
3. Evaluation with public benchmarks to show the superiority of the proposed approach.

Related Work

Deep Learning approaches for tabular data:

While gradient boosted decision trees (GBDTs) remain the state-of-the-art approach for tabular data analysis, the deep learning community has made significant progress in this domain. Models such as TabNet(Arik and Pfister 2021), Neural Oblivious Decision Trees(NODE)(Popov, Morozov, and Babenko 2020), FT-Transformer(Gorishniy et al. 2021), Net-DNF(Katzir, Elidan, and El-Yaniv 2021) and DANet(Chen et al. 2021) have demonstrated competitive performance, often outperforming or matching the popular "shallow" GBDT models.

NODE(Popov, Morozov, and Babenko 2020) combined neural oblivious decision trees with dense connections and achieved comparable performance to GBDTs. Net-DNF(Katzir, Elidan, and El-Yaniv 2021) employed soft versions of logical boolean formulas to aggregate results from numerous shallow fully-connected models. NODE and Net-DNF followed ensemble learning approaches, utilizing a

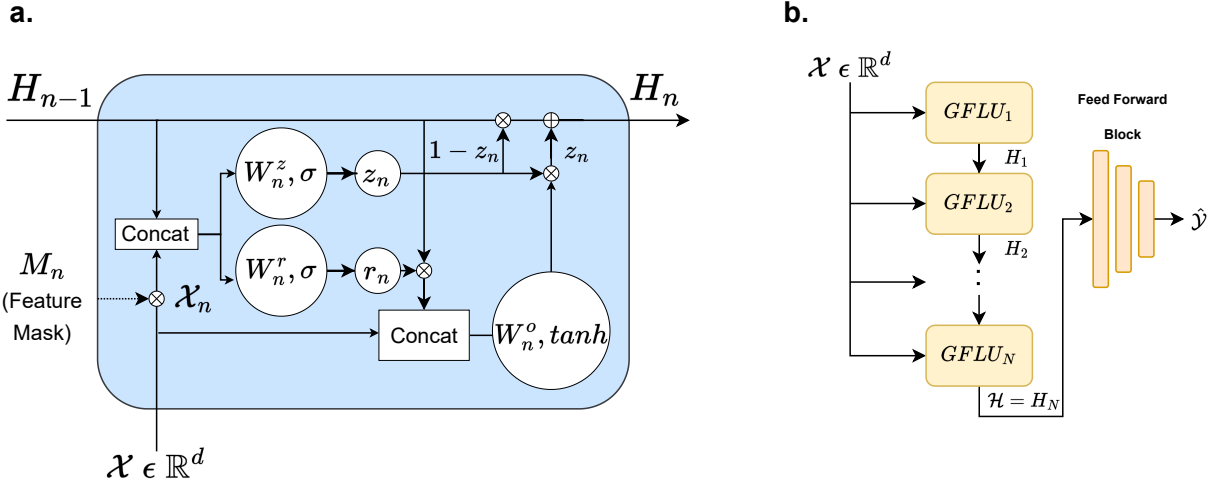


Figure 1: a. Detailed View of the Gated Feature Learning Unit. \otimes represents element wise multiplication and \oplus addition, b. Overall Architecture of GANDALF

large number of shallow networks, resulting in high computational complexity. TabNet(Arik and Pfister 2021) sequentially computed sparse attentions to mimic the feature splitting procedure of tree models. But TabNet has been shown to have inferior performance by Katzir, Elidan, and El-Yaniv (2021) and Borisov et al. (2022).

Feature Representation Learning: Tabular data has well-defined features, but data scientists still spend a lot of time curating and creating new features. This shows the need for representation learning that can automate feature selection and feature interactions.

Classical decision trees use information metrics, such as Gini index, for feature selection while fully connected networks consider all the features and their interactions. This makes Decision Trees less prone to the noise. TabNet(Arik and Pfister 2021) uses an attention mechanism for feature selection, but it operates at the instance level. NODE(Popov, Morozov, and Babenko 2020) uses learnable feature masks with the α -entmax function(Peters, Niculae, and Martins 2019) for feature selection within the context of the oblivious trees. DANet(Chen et al. 2021) also uses the α -entmax function as feature masks and uses batch normalization along with learnable weights in a simple attention mechanism to learn representations. In this work, we use a similar approach to DANet but avoid the need for batch normalization and introduce learnable sparsity in the proposed novel gating mechanism.

Gating Mechanism: Gating mechanisms have gained significant popularity in deep learning for their ability to control the information flow within a network. These mechanisms have been widely applied across various domains, including computer vision, natural language processing (NLP), recommendation systems, and even tabular data analysis. In sequence models like LSTM(Hochreiter and Schmidhuber 1997), GRU(Cho et al. 2014), and Highway Networks(Srivastava, Greff, and Schmidhuber 2015), gating

mechanisms are commonly employed to mitigate issues like vanishing and exploding gradients. Another notable component that incorporates gating is Gated Linear Units(Dauphin et al. 2017; Gehring et al. 2017), which has found applications in language modeling and machine translation.

Gated Adaptive Network for Deep Automated Learning of Features (GANDALF)

Feature Selection, and Feature Engineering are considered to be essential for SOTA performance in tabular datasets. GANDALF is specifically designed with these principles in mind. The gating mechanism in GANDALF acts as a barrier against noisy data, just like Gandalf from *Lord of the Rings*(LOTR) who stood on top of a narrow bridge in the Mines of Moria and commanded *Balrog*, a powerful demonic monster, with all his might and power - *"You shall not pass"*.

Suppose we have a training dataset, $\mathcal{D} = (\mathcal{X}, \mathcal{Y}) = \{(x_i, y_i)\}_{i=1}^S$, where each $x_i \in \mathbb{R}^d$ is a d -dimensional data with a corresponding label $y_i \in \mathcal{Y}$. We assume all the input features are numerical to make notations simpler. Any categorical feature can be encoded using sufficient preprocessing or a learnable embedding layer, as is the norm in tabular data. For classification problems, $\mathcal{Y} = \{1, \dots, K\}$ and for regression $\mathcal{Y} \in \mathbb{R}$.

There are two main stages in the GANDALF. The input features, $\mathcal{X} \in \mathbb{R}^d$, is first processed by a series of Gated Feature Learning Units (GFLU). The GFLUs learn the best representation of the input features by feature selection and feature interactions. This learned representation is then processed using a simple Feed Forward Network to produce the final prediction.

Gated Feature Learning Units (GFLU)

Gated Feature Learning Unit is an architecture which is inspired by the gating flows in Gated Recurrent Units(Cho et al.

2014), but adapted for hierarchical feature learning for tabular data with key modifications. GFLU performs two functions - automated feature selection and feature engineering. And by stacking multiple GFLUs on top of each other, we facilitate hierarchical learning of the optimal representation for the task it is trained for. We denote the stage of the GFLU by n . The key difference between a GFLU and a GRU is in the way we use a learnable feature mask to softly select a subset of features as the input to the GFLU at each stage and thereby making the inputs to the different GFLUs, which are stacked on top of each other, different. *Figure 1* shows a single Gated Feature Learning Unit. We can think of GFLUs selecting what information to use from the raw features and using its internal mechanism to learn and unlearn to create the best set of features which is required for the task. The aim of this module is to learn a function $F : \mathbb{R}^d \rightarrow \mathbb{R}^{\tilde{d}}$. Although we can use the hidden state dimensions to increase or decrease the dimensions of the learned feature representation (\tilde{d}), we have chosen to keep it the same in all our experiments.

Feature Selection: We use a learnable mask $\mathbf{M}_n \in \mathbb{R}^d$ for the soft selection of important features for each stage, n , of feature learning in the GFLU. The mask is constructed by applying a sparse transformation on a learnable parameter vector ($\mathbf{F}_n \in \mathbb{R}^d$).

In order to encourage sparsity, we propose to use the t -softmax (Bałazy et al. 2023). They proposed a weighted softmax, as a general form of the softmax.

$$\text{softmax}(a_i, w_i) = \frac{w_i \exp(a_i)}{\sum_{j=1}^n w_j \exp(a_j)} \quad (1)$$

where a_i is the i -th term in the vector over which we are applying the activation, and w_i is the corresponding weight. Under this formulation, if the weight of any term becomes zero ($W_i = 0$), the resulting activated value would also be zero ($\text{softmax}(a_i, w_i) = 0$). To make this parameterization easier, they proposed t-softmax, which made all the weights depend on a single parameter, $t > 0$.

$$\begin{aligned} t\text{-softmax}(a, t) &= \text{softmax}(a, w_t), \\ \text{where } w_t &= \text{ReLU}(a_t + t - \max(a)) \end{aligned} \quad (2)$$

We can see that all the weights, w_i , are positive and at least 1 would be non-zero. This operation is almost as fast as the regular softmax and does not suffer from computational inefficiencies like other sparse activations (α -entmax (Peters, Niculae, and Martins 2019) and sparsemax (Martins and Astudillo 2016)) which require a sorting operation.

The proposed masking in the GFLU is multiplicative. Formally this feature selection is defined by:

$$M_n = t\text{-softmax}(\mathbf{F}_n, t) \quad (3)$$

$$\mathcal{X}_n = M_n \odot \mathcal{X} \quad (4)$$

where $\mathcal{X}_n \in \mathbb{R}^d$ is the input features (after feature selection) and $\mathbf{M}_n = t\text{-softmax}(\mathbf{F}_n)$ and \odot denotes an element-wise multiplication operation. In the t -softmax, t can be a learnable parameter or non-learnable. When it is set to non-learnable, proper initialization of the parameter t is essential. We will go deeper into initialization strategies later. If the parameter, t , is learnable, proper initialization is not essential, but helpful.

Gating Mechanism The gating mechanism, which is inspired by Gated Recurrent Units, has a reset and update gate. The feature selection using the masks is only used for the gates, and not for the candidate at stage n . At any stage, n , it takes as an input, $\mathcal{X} \in \mathbb{R}^d$ & $H_{n-1} \in \mathbb{R}^{\tilde{d}}$ as an input and learns a feature representation, $H_n \in \mathbb{R}^{\tilde{d}}$. *Figure 1* shows the schematic of a GFLU.

Instead of the hidden state that a GRU maintains to learn from a sequence, a GFLU learns a hidden feature representation. Another key difference between the standard GRU and GFLU is that the weights are not shared between different stages. While the GRU wants to learn a single function given an input window, we want the GFLU to learn different functions for each stage so that they can be hierarchically stacked to create good feature representations.

At any stage, n , the hidden feature representation is a linear interpolation between previous feature representation(H_{n-1}) and current candidate feature representation(\tilde{H}_n)

$$H_n = (1 - z_n) \odot H_{n-1} + z_n \odot \tilde{H}_n \quad (5)$$

where z_n is the update gate which decides how much information to use to update its internal feature representation. The update gate is defined as

$$z_n = \sigma(W_n^z \cdot [H_{n-1}; \mathcal{X}_n]) \quad (6)$$

where $[H_{n-1}; \mathcal{X}_n]$ represents a concatenation operation between H_{n-1} and \mathcal{X}_n , σ is the sigmoid activation function, and W_n^z is a learnable parameter.

The candidate feature representation(\tilde{H}_n) is computed as

$$\tilde{H}_n = \tanh(W_n^o \cdot [r_n \odot H_{n-1}; \mathcal{X}]) \quad (7)$$

where r_n is the reset gate which decides how much information to forget from previous feature representation, W_n^o is a learnable parameter, $[\cdot]$ represents a concatenation operation, and \odot represents element-wise multiplication. Note that we are using the original feature, \mathcal{X} , and not the masked feature, \mathcal{X}_n . This design decision helps the information to flow freely through the GFLU hidden states.

The reset gate (r_n) is computed similar to the update gate

$$r_n = \sigma(W_n^r \cdot [H_{n-1}; \mathcal{X}_n]) \quad (8)$$

In practice, we can use a single matrix ($W_n^i \in \mathbb{R}^{2d \times 2d}$) to compute the reset and update gates together to save some computation. We can stack any number of such GFLUs to encourage hierarchical learning of features and the feature representation from the last GFLU stage, $\mathcal{H} \in \mathbb{R}^{\tilde{d}}$, is used in the subsequent stages.

Network Architecture and Initialization

GANDALF is a stack of N GFLUs arranged in a sequential manner, each stage, n , selecting a subset of features and learning a representation of features, and multiple stages acting in a hierarchical way to build up the optimal representation (\mathcal{H}) for the task at hand. Now this representation (\mathcal{H}) is fed to a standard K Layer Feed Forward Network with non-linear activations (ReLU).

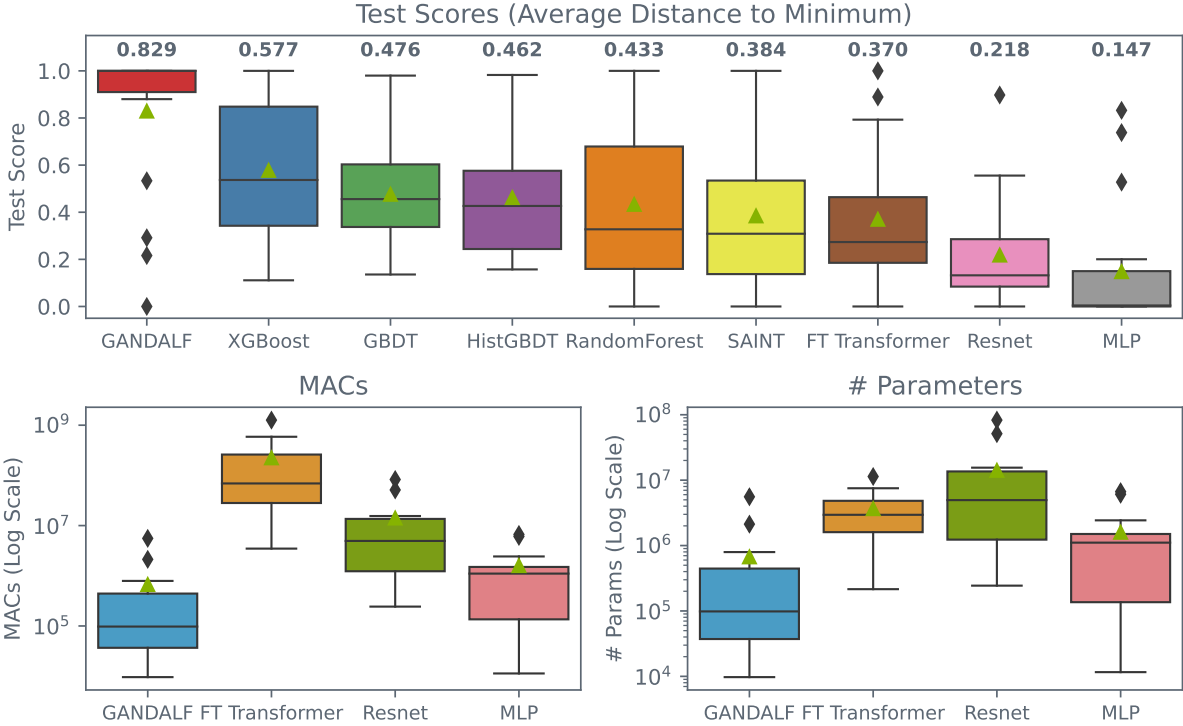


Figure 2: Benchmarking on Tabular Benchmark Grinsztajn, Oyallon, and Varoquaux (2022). The box plot of the normalized test scores across datasets show that GANDALF consistently achieve the best scores. The box plots of the number of parameters and MACs show that GANDALF achieves the high performance with higher parameter efficiency and computational efficiency.

$$\text{Classification: } \hat{\mathcal{Y}} = f(\mathcal{H}; W_1, b_1, \dots, W_K, b_K) \quad (9)$$

$$\text{Regression: } \hat{\mathcal{Y}} = T_0 + f(\mathcal{H}; W_1, b_1, \dots, W_K, b_K) \quad (10)$$

where $W_1, b_1, \dots, W_K, b_K$ are the weights and biases of the K layer Feed Forward Network and T_0 is the average label/target value, which is initialized from training data. T_0 makes the model robust to the scale of the label, \mathcal{Y} , in case of regression.

Initialization is how we can inject our priors into the architecture. We want each of stage, n , to have a different view of the features to encourage diversity in the hierarchical feature representation learning. At the same time, we also want the feature selection to be sparse. Therefore we initialize F_n from different Beta distributions with its two parameters (α_n and β_n) randomly sampled from a uniform distribution [0.5, 10].

Bałazy et al. (2023) had also proposed another variant of the softmax, r -softmax where the expected sparsity can be plugged into the activation by using an intuitive parameter they call the sparsity rate, r .

$$r\text{-softmax}(x, r) = t\text{-softmax}(x, t_r), \quad (11)$$

where $t = -\text{quantile}(x, r) + \max(x)$

We don't use this directly in the GFLU because the quantile operation is a costly operation. But instead, we use this as a way to initialize the t parameter at the start of training. This is a hyperparameter of the architecture with which we can

inject our prior belief about the amount of noise in the input data. Even if the initialization is not spot-on, the network still adjusts itself through training to the right value of t .

Experiments and Analysis

In this section, we report the comparison of GANDALF with other models using two publicly available and large-scale benchmarks - *Tabular Benchmark*(Grinsztajn, Oyallon, and Varoquaux 2022) & *TabSurvey*(Borisov et al. 2022)- along with insights into the hyperparameters and interpretability of GANDALF. All experiments used PyTorch Tabular(Joseph 2021) and were run on a single NVIDIA RTX 3060 with 20 cores and 16GB of RAM. The batch size was fixed at 512 for all experiments except *Higgs* dataset for the *TabSurvey* benchmark. For *Higgs*, we used a 4096 as the batchsize, along with mixed precision training and sub-epoch level checkpointing to make the runs faster.

Comparison with Public Benchmarks

The selection of datasets to benchmark is not standard in the tabular domain. However, there are now some open benchmarks that provide a standard set of datasets and evaluation metrics. We use these benchmarks to make our evaluation transparent and comparable to other work. We do not re-run the models that the benchmarks already tested, but we do evaluate GANDALF the same way as in the benchmark.

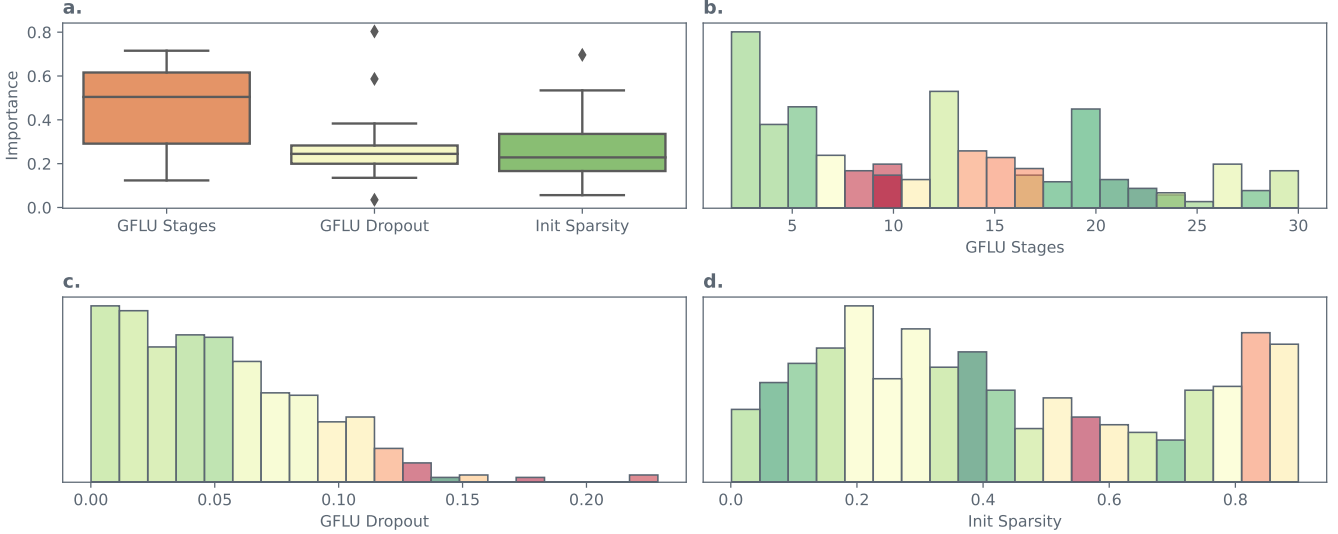


Figure 3: Hyperparameter Study. a. The box plot of hyperparameter importances across 18 datasets. b - d. Histograms of hyperparameters where each bin is colored according to the average test scores in that bin. Green is higher and Red is lower.

We use Optuna library(Akiba et al. 2019) to run Bayesian Optimization (BO) with Tree Parzen Estimator(Bergstra et al. 2011) for 100 trials. We stick to the open benchmarks for the train-test splits, pre-processing, cross validation folds, and the metrics used. We report the average score on test split for *Tabular Benchmark* and on the validation split for *TabSurvey*, as is done in these respective benchmarks. Wherever we have run more than 1 folds, we also report the standard deviation of the scores.

We also use *Thop*(Zhu 2013) to calculate the number of parameters and MACs for the best performing deep learning models and report them. When aggregating across different datasets, we have used the average distance to the minimum (ADTM) metric (Wistuba, Schilling, and Schmidt-Thieme 2015; Grinsztajn, Oyallon, and Varoquaux 2022). It is a simple affine transformation which scales the performances between 0 and 1. $ADTM(s \in S) = \frac{s - \min(S)}{\max(S) - \min(S)}$, where S is all the scores of best models in a dataset. In *TabSurvey*, regression is measured using mean squared error, which is a lower-is-better metric and we adapted ADTM to be $ADTM(s \in S) = \frac{s - \max(S)}{\max(S) - \min(S)}$ to be consistent with the interpretation.

Tabular Benchmark *Tabular Benchmark* used 45 datasets from varied domains, carefully curated to capture the variety of tabular datasets and made publically available thorough OpenML(Bischl et al. 2017). They ran separate benchmarking for numerical and categorical classification/regression, medium and large sized datasets, with and without target transforms, data transforms, etc., accounting for more than 20,000 compute hours. To limit our computational burden and make the evaluation on datasets resembling real-world problems, we have selected a subset of 18 datasets and benchmarks from this according to the following rules:

1. Only medium sized datasets, i.e. maximum size of all the

datasets is 10000

2. No target or data transformations
3. Only datasets with more than 20 features
4. If a dataset was used for both numerical and categorical benchmarks, we chose the categorical benchmark.

Figure 2 shows the box plots of the normalized test scores across datasets and the number of parameters and MACs for deep learning models. Detailed results available in the Appendix.

Tabsurvey Benchmark

We also used a smaller benchmark, with just 5 datasets, to ensure larger coverage on existing tabular models. The benchmark covers 20 models, 12 from Deep Learning. We excluded *Heloc* dataset because the processed dataset wasn't available publicly. We used the same definition of ADTM to aggregate scores across the four datasets and the results are plotted in Figure 5. Detailed results available in the Appendix.

Hyperparameter Study

GANDALF has a very expressive architecture with very minimal hyperparameters. There are only three key hyperparameters - # of *GFLU Stages*, *Dropout in each GFLU*, and *Init Sparsity*. For all our experiments, we kept the dimensions of the Feed Forward network constant with two hidden layers of 32 and 16 units respectively with a ReLU activation, and set the sparsity parameter as learnable. Hyperparameter search was done on the below search space for 100 trials using BO,

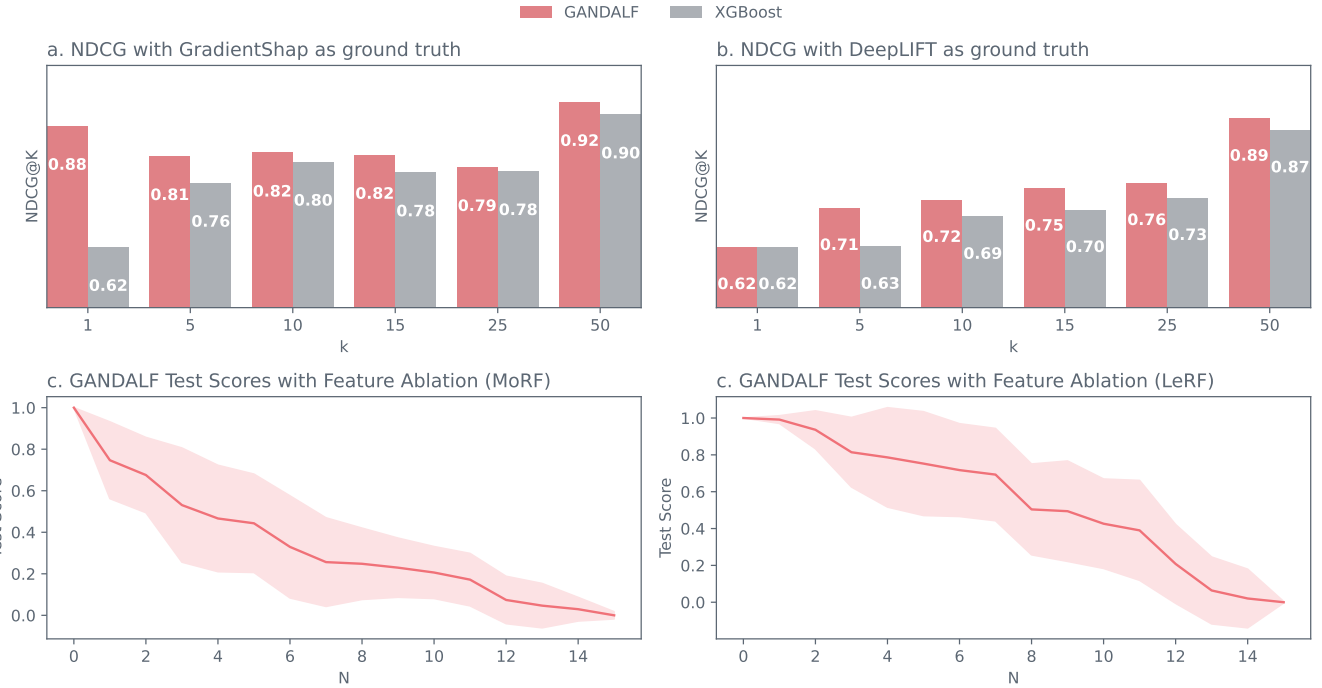


Figure 4: Interpretability Study. a-b. The NDCG@K scores for GANDALF and XGBoost Feature importance against GradientSHAP and DeepLIFT. c-d. Median normalized test scores in feature ablation trials for Most Relevant First (MoRF) and Least Relevant First (LoRF) strategies.

with first 10 trials as pure random exploration.

$$GFLU \text{ Stages} \in \{2, 3, \dots, 30\}$$

$$GFLU \text{ Dropout} \sim \text{Uniform}(0.0, 0.5)$$

$$\text{Init Sparsity} \sim \text{Uniform}(0.0, 0.9)$$

$$\text{Weight Decay} \in \{10^{-3}, 10^{-4}, 10^{-5}, 10^{-6}, 10^{-7}, 10^{-8}\}$$

$$\text{Learning Rate} \in \{10^{-3}, 10^{-4}, 10^{-5}, 10^{-6}\}$$

We should notice that the only architecture specific hyperparameter that was tuned was the # of GFLU stages and GFLU Dropout. To study how fast the tuning converges, we ran simulated scenarios where identified the best performing model among all models if we had run only T trials, where $T \in 1, 2, \dots, 20$. Out of 18 datasets in *Tabular Benchmark*, GANDALF was the best performing model in 13 of them as early as 5 trials (where we are still in the random exploration phase). Figure 6 in Appendix shows the detailed plot.

We conducted an in-depth analysis of hyperparameter tuning across 18 datasets to identify crucial parameters and establish effective default ranges for tuning. We used the Optuna implementation of FANOVA (Hutter, Hoos, and Leyton-Brown 2014) to assess the relative importance of each hyperparameter. To isolate the influence of Learning Rate and Weight Decay, we focused exclusively on trials utilizing the optimal values for these parameters. We also plotted the histogram of trial values for # of GFLU Stages, GFLU Dropout, and Init Sparsity and colored each bin based on the average normalized test score to give an indication of the possible ranges of the hyperparameters.

Figure 3 shows the corresponding plots. The key observations are:

1. Even though the sparsity parameter is learnable, giving it a good starting point helps quite a bit. But we can see that a sparsity between 0.0 and 0.5 is a good range to search.
2. *GFLU Dropout* has its sweet spot between 0 and 0.05. This can also be because the *GFLU Dropout* is applied to each GFLU stage and hence compounding the effect.
3. # of *GFLU Stages* doesn't show any particular pattern, but is having the highest impact on performance. This tells us tuning the # of *GFLU Stages* is essential.

Interpretability

By virtue of the design, GANDALF comes with interpretability. The learned feature masks of each stage of the GFLU serves as an indicator on how much the model is relying on a feature for the task and we can combine them into an aggregate representation as shown in Eqn: 12. If we want to limit the range between 0 and 1, we can just normalize it as well.

$$\mathcal{I} = \sum_{n=1}^N M_n \quad \mathcal{I}_i^{\text{norm}} = \frac{\mathcal{I}_i}{\sum_{i=1}^D \mathcal{I}_i} \quad (12)$$

where N is the number of GFLU stages, and D is the number of features in \mathcal{X} . This can be seen similar to the feature importance that we get from popular GBDT implementations. We carried out two experiments to analyze the interpretability

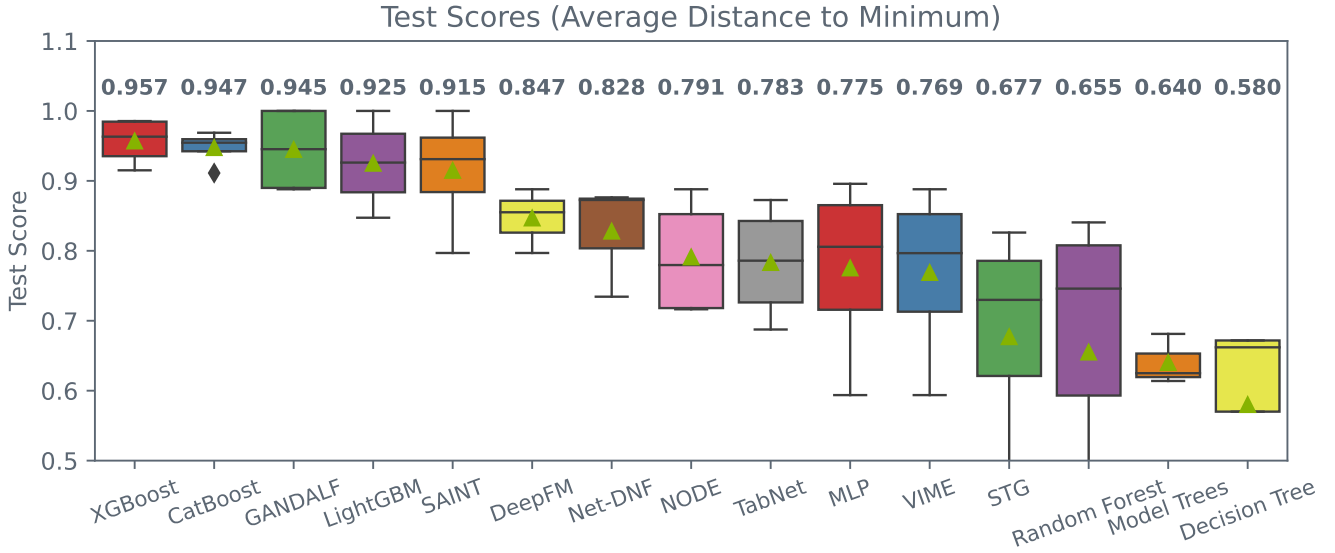


Figure 5: Benchmarking on TabSurvey(Borisov et al. 2022). The box plot of the normalized test scores across 4 datasets shows GANDALF being at par with GBDTs and better than other DL models.

features of GANDALF. For both experiments, we only used datasets from the *Tabular Benchmark* which has no categorical features. This was done only to make the analysis simpler. In case of categorical features, we will just need to average the \mathcal{I} s associated with the corresponding embeddings.

Ranking Metrics of the Feature Importance Evaluating feature attributions or importance is not a trivial task. Since there is no ground truth for checking the quality of interpretability, we decided to use GradientSHAP(Lundberg and Lee 2017) and DeepLIFT(Shrikumar, Greenside, and Kundaje 2017) as a measure of ground truth.

We formulated the assessment as a recommendation problem where the ground truth is the top 25 features according to GradientSHAP and DeepLIFT. We compare the ranked feature importance from best performing configurations of GANDALF and XGBoost (as a baseline) using $NDCG@K$ (Järvelin and Kekäläinen 2002) at different values of $K \in \{1, 5, 10, 15, 25, 50\}$.

Figure 4a and *Figure 4b* plots show the results. We can see that the NDCG scores of the *GANDALF* feature importance are consistently better than the baseline, *XGBoost*, when compared against GradientSHAP and DeepLIFT ground truths. This shows that the GANDALF feature importance is at least as good as the popularly used alternative for GBDTs.

Feature Ablation Study Another quantifiable aspect of an explanation is it's *fidelity*. *Fidelity* measures how well an explanation represents the processing performed by a model on its inputs to produce the output. If a feature importance ranking is true, then if we perturb the information in each feature from most relevant features first (MoRF) (Tomsett et al. 2020), the performance of the model should decrease rapidly. And if we do it in the reverse order, Least Relevant First (LeRF), we should not expect huge drops in performance.

Borisov et al. (2022) also uses this technique to assess the fidelity of the feature attributions. But they removed the feature and retrained the model without the feature. We chose to keep the model the same and replaced each feature with gaussian noise as a perturbation. Retraining the model without the feature can also change the way the model is configured and may not measure the fidelity of the model we are interested in anymore.

Figure 4b and *Figure 4c* plots show the *MoRF* and *LeRF* curves for GANDALF feature importance. We can see that as expected, the performance drops sharply when we remove most relevant features first (MoRF) and it falls less rapidly when we remove least relevant features first(LeRF).

Conclusion

We have proposed Gated Adaptive Network for Deep Automated Learning of Features (GANDALF), a novel deep learning architecture for tabular data. GANDALF relies on a novel gating mechanism as a feature representation learning unit (GFLU) with an in-built feature selection mechanism. GANDALF stands tall in front of noisy datasets and proclaim “*You shall not pass*” to non-informative features, hence named after the great Wizard from Lord of the Rings. The proposed GFLU unit can also be thought of as a modular and composable unit which is tailor-made to process tabular data. Experiments on multiple public benchmarks verified that GANDALF is a competitive alternative to the popular GBDT models, and comes with it the added benefit of being explainable out-of-the-box. With very few architecture specific hyperparameters and fast training, finding the best hyperparameters for a task is made easier. We have made available the code at https://github.com/manujosephv/pytorch_tabular under MIT License.

References

Akiba, T.; Sano, S.; Yanase, T.; Ohta, T.; and Koyama, M. 2019. Optuna: A Next-generation Hyperparameter Optimization Framework. *Knowledge Discovery And Data Mining*.

Arik, S. Ö.; and Pfister, T. 2021. TabNet: Attentive Interpretable Tabular Learning. In *AAAI*, volume 35, 6679–6687.

Bałazy, K.; Łukasz Struski; Śmieja, M.; and Tabor, J. 2023. r-softmax: Generalized Softmax with Controllable Sparsity Rate. *arXiv preprint arXiv: 2304.05243*.

Bergstra, J.; Bardenet, R.; Bengio, Y.; and Kégl, B. 2011. Algorithms for Hyper-Parameter Optimization. In Shawe-Taylor, J.; Zemel, R.; Bartlett, P.; Pereira, F.; and Weinberger, K., eds., *Advances in Neural Information Processing Systems*, volume 24. Curran Associates, Inc.

Bischl, B.; Casalicchio, G.; Feurer, M.; Hutter, F.; Lang, M.; Mancovani, R.; Rijn, J. N.; and Vanschoren, J. 2017. OpenML Benchmarking Suites. *Neurips Datasets And Benchmarks*.

Borisov, V.; Leemann, T.; Seßler, K.; Haug, J.; Pawelczyk, M.; and Kasneci, G. 2021. Deep Neural Networks and Tabular Data: A Survey. *arXiv preprint arXiv: Arxiv-2110.01889*.

Borisov, V.; Leemann, T.; Seßler, K.; Haug, J.; Pawelczyk, M.; and Kasneci, G. 2022. Deep Neural Networks and Tabular Data: A Survey. *IEEE Transactions on Neural Networks and Learning Systems*, PP: 1–21.

Chen, J.; Liao, K.-Y.; Wan, Y.; Chen, D.; and Wu, J. 2021. DANets: Deep Abstract Networks for Tabular Data Classification and Regression. *Aaaai Conference On Artificial Intelligence*.

Chen, T.; and Guestrin, C. 2016. XGBoost: A Scalable Tree Boosting System. In *Proceedings of the 22nd ACM SIGKDD International Conference on Knowledge Discovery and Data Mining*, KDD ’16, 785–794. New York, NY, USA: Association for Computing Machinery. ISBN 9781450342322.

Cho, K.; van Merriënboer, B.; Bahdanau, D.; and Bengio, Y. 2014. On the Properties of Neural Machine Translation: Encoder–Decoder Approaches. In *Proceedings of SSST-8, Eighth Workshop on Syntax, Semantics and Structure in Statistical Translation*, 103–111. Doha, Qatar: Association for Computational Linguistics.

Dauphin, Y. N.; Fan, A.; Auli, M.; and Grangier, D. 2017. Language Modeling with Gated Convolutional Networks. In Precup, D.; and Teh, Y. W., eds., *Proceedings of the 34th International Conference on Machine Learning, ICML 2017, Sydney, NSW, Australia, 6-11 August 2017*, volume 70 of *Proceedings of Machine Learning Research*, 933–941. PMLR.

Devlin, J.; Chang, M.-W.; Lee, K.; and Toutanova, K. 2019. BERT: Pre-training of Deep Bidirectional Transformers for Language Understanding. In *Proceedings of the 2019 Conference of the North American Chapter of the Association for Computational Linguistics: Human Language Technologies, Volume 1 (Long and Short Papers)*, 4171–4186. Minneapolis, Minnesota: Association for Computational Linguistics.

Friedman, J. H. 2001. Greedy Function Approximation: A Gradient Boosting Machine. *The Annals of Statistics*, 29(5): 1189–1232.

Gehring, J.; Auli, M.; Grangier, D.; Yarats, D.; and Dauphin, Y. N. 2017. Convolutional Sequence to Sequence Learning. In Precup, D.; and Teh, Y. W., eds., *Proceedings of the 34th International Conference on Machine Learning, ICML 2017, Sydney, NSW, Australia, 6-11 August 2017*, volume 70 of *Proceedings of Machine Learning Research*, 1243–1252. PMLR.

Goodfellow, I.; Bengio, Y.; and Courville, A. 2016. *Deep Learning*. MIT Press. <http://www.deeplearningbook.org>.

Gorishniy, Y.; Rubachev, I.; Khrulkov, V.; and Babenko, A. 2021. Revisiting Deep Learning Models for Tabular Data. In Ranzato, M.; Beygelzimer, A.; Dauphin, Y. N.; Liang, P.; and Vaughan, J. W., eds., *Advances in Neural Information Processing Systems 34: Annual Conference on Neural Information Processing Systems 2021, NeurIPS 2021, December 6-14, 2021, virtual*, 18932–18943.

Grinsztajn, L.; Oyallon, E.; and Varoquaux, G. 2022. Why do tree-based models still outperform deep learning on tabular data? *ArXiv*, abs/2207.08815.

Hochreiter, S.; and Schmidhuber, J. 1997. Long Short-term Memory. *Neural computation*, 9: 1735–80.

Hutter, F.; Hoos, H.; and Leyton-Brown, K. 2014. An Efficient Approach for Assessing Hyperparameter Importance. In Xing, E. P.; and Jebara, T., eds., *Proceedings of the 31st International Conference on Machine Learning*, volume 32 of *Proceedings of Machine Learning Research*, 754–762. Bejing, China: PMLR.

Järvelin, K.; and Kekäläinen, J. 2002. Cumulated Gain-Based Evaluation of IR Techniques. *ACM Trans. Inf. Syst.*, 20(4): 422–446.

Joseph, M. 2021. PyTorch Tabular: A Framework for Deep Learning with Tabular Data. *arXiv preprint arXiv: Arxiv-2104.13638*.

Katzir, L.; Elidan, G.; and El-Yaniv, R. 2021. Net-{DNF}: Effective Deep Modeling of Tabular Data. In *International Conference on Learning Representations*.

Ke, G.; Meng, Q.; Finley, T.; Wang, T.; Chen, W.; Ma, W.; Ye, Q.; and Liu, T.-Y. 2017. LightGBM: A Highly Efficient Gradient Boosting Decision Tree. In Guyon, I.; Luxburg, U. V.; Bengio, S.; Wallach, H.; Fergus, R.; Vishwanathan, S.; and Garnett, R., eds., *Advances in Neural Information Processing Systems*, volume 30. Curran Associates, Inc.

Krizhevsky, A.; Sutskever, I.; and Hinton, G. E. 2017. ImageNet Classification with Deep Convolutional Neural Networks. *Commun. ACM*, 60(6): 84–90.

Lundberg, S. M.; and Lee, S.-I. 2017. A Unified Approach to Interpreting Model Predictions. In Guyon, I.; Luxburg, U. V.; Bengio, S.; Wallach, H.; Fergus, R.; Vishwanathan, S.; and Garnett, R., eds., *Advances in Neural Information Processing Systems*, volume 30. Curran Associates, Inc.

Martins, A. F. T.; and Astudillo, R. F. 2016. From Softmax to Sparsemax: A Sparse Model of Attention and Multi-Label Classification. In *Proceedings of the 33rd International Conference on International Conference on Machine Learning - Volume 48*, ICML’16, 1614–1623. JMLR.org.

Peters, B.; Niculae, V.; and Martins, A. F. T. 2019. Sparse Sequence-to-Sequence Models. In *Proceedings of the 57th Annual Meeting of the Association for Computational Linguistics*, 1504–1519. Florence, Italy: Association for Computational Linguistics.

Popov, S.; Morozov, S.; and Babenko, A. 2020. Neural Oblivious Decision Ensembles for Deep Learning on Tabular Data. In *8th International Conference on Learning Representations, ICLR 2020, Addis Ababa, Ethiopia, April 26-30, 2020*. OpenReview.net.

Prokhorenkova, L.; Gusev, G.; Vorobev, A.; Dorogush, A. V.; and Gulin, A. 2018. CatBoost: unbiased boosting with categorical features. In Bengio, S.; Wallach, H.; Larochelle, H.; Grauman, K.; Cesa-Bianchi, N.; and Garnett, R., eds., *Advances in Neural Information Processing Systems*, volume 31. Curran Associates, Inc.

Shrikumar, A.; Greenside, P.; and Kundaje, A. 2017. Learning Important Features Through Propagating Activation Differences. *International Conference On Machine Learning*.

Shwartz-Ziv, R.; and Armon, A. 2022. Tabular data: Deep learning is not all you need. *Inf. Fusion*, 81: 84–90.

Silver, D.; Huang, A.; Maddison, C. J.; Guez, A.; Sifre, L.; van den Driessche, G.; Schrittwieser, J.; Antonoglou, I.; Panneershelvam, V.; Lanctot, M.; Dieleman, S.; Grewe, D.; Nham, J.; Kalchbrenner, N.; Sutskever, I.; Lillicrap, T.; Leach, M.; Kavukcuoglu, K.; Graepel, T.; and Hassabis, D. 2016. Mastering the game of Go with deep neural networks and tree search. *Nature*, 529(7587): 484–489.

Srivastava, R. K.; Greff, K.; and Schmidhuber, J. 2015. Highway Networks. *ArXiv*, abs/1505.00387.

Tomsett, R.; Harborne, D.; Chakraborty, S.; Gurram, P.; and Preece, A. 2020. Sanity Checks for Saliency Metrics. *Proceedings of the AAAI Conference on Artificial Intelligence*, 34(04): 6021–6029.

Wistuba, M.; Schilling, N.; and Schmidt-Thieme, L. 2015. Learning hyperparameter optimization initializations. In *2015 IEEE International Conference on Data Science and Advanced Analytics (DSAA)*, 1–10.

Zhu, L. 2013. THOP: PyTorch-OpCounter. <https://github.com/Lyken17/pytorch-OpCounter>.

Appendix: Additional Tables and Figures

Table 1: Summary of datasets from Tabular Benchmark(Grinsztajn, Oyallon, and Varoquaux 2022) used in the experiments.

Benchmark	Dataset	Type	# Folds	# Features	Train Size	Test Size
Categorical Classification	albert	Classification	1	31	10000	33777
Categorical Classification	covertype	Classification	1	54	10000	50000
Categorical Classification	default-credit-card	Classification	3	21	9290	2788
Categorical Classification	eye_movements	Classification	3	23	5325	1599
Categorical Classification	road-safety	Classification	1	32	10000	50000
Categorical Regression	Allstate	Regression	1	124	10000	50000
Categorical Regression	Mercedes	Regression	5	359	2946	885
Categorical Regression	topo_2_1	Regression	3	255	6219	1867
Numeric Classification	Bioresponse	Classification	5	419	2403	722
Numeric Classification	Higgs	Classification	1	24	10000	50000
Numeric Classification	MiniBooNE	Classification	1	50	10000	44099
Numeric Classification	heloc	Classification	3	22	7000	2100
Numeric Classification	jannis	Classification	1	54	10000	33306
Numeric Classification	pol	Classification	3	26	7057	2118
Numeric Regression	Ailerons	Regression	3	33	9625	2888
Numeric Regression	cpu_act	Regression	3	21	5734	1721
Numeric Regression	superconduct	Regression	1	79	10000	7885
Numeric Regression	yprop_4_1	Regression	3	42	6219	1867

Table 2: Summary of datasets from Tab Survey(Borisov et al. 2022) used in the experiments.

Dataset	Type	Categorical Features	# Folds	# Features	Train Size	Test Size
adult-income	Classification	True	1	14	22792	9769
Higgs	Classification	True	1	28	7700000	3300000
covertype	Classification	False	1	54	406708	174304
california-housing	Regression	False	2	8	14448	6192

Table 3: Test scores on Tabular Benchmark(Grinsztajn, Oyallon, and Varoquaux 2022). For classification Accuracy and for regression R^2 score is reported. The best performing model is highlighted in bold.

Dataset	GANDALF	XGBoost	HistGBDT	GBDT	RandomForest	FT Transformer	Resnet	SAINT	MLP
albert	68.53	65.70	65.78	65.76	65.53	65.63	65.23	65.52	65.32
covertype	93.22	86.58	84.98	85.43	85.86	85.93	83.96	85.33	83.32
default-credit-card	72.80	72.08	72.00	72.09	72.13	71.90	71.40	71.90	71.41
eye_movements	67.89	66.85	64.23	64.67	66.21	60.00	59.97	60.56	60.54
road-safety	80.88	76.89	76.42	76.31	76.13	77.09	76.09	76.69	75.59
Allstate	59.11	53.65	52.74	53.04	49.70	52.01	51.41	52.60	51.58
Mercedes	59.84	57.87	57.89	57.76	57.81	56.63	57.29	56.45	55.91
topo_2_1	4.85	6.94	7.31	5.34	7.36	5.33	5.06	6.05	4.15
Bioresponse	88.16	79.31	-	78.59	79.86	75.82	77.06	76.87	76.70
Higgs	75.23	71.37	-	71.04	70.93	70.61	69.48	70.82	68.97
MiniBooNE	92.42	93.72	-	93.44	92.72	93.51	93.67	93.81	93.45
heloc	72.26	72.16	-	72.35	72.10	72.67	72.41	72.37	72.40
jannis	79.35	78.03	-	77.47	77.30	76.83	75.37	77.12	74.57
pol	98.98	98.33	-	98.16	98.24	98.50	95.22	98.21	94.70
Ailerons	86.46	83.66	84.49	83.43	-	73.28	71.85	70.10	83.72
cpu_act	98.29	98.62	98.35	98.61	-	98.48	98.26	98.51	97.91
superconduct	92.57	91.06	90.16	90.32	-	89.03	89.53	-	89.65
yprop_4_1	8.53	8.29	-	5.57	9.39	5.35	4.28	5.95	2.23

Table 4: Standard deviation of test scores on Tabular Benchmark Grinsztajn, Oyallon, and Varoquaux (2022) (Only Datasets where k-Fold Validation was carried out). For classification Accuracy and for regression R^2 score is reported.

Dataset	GANDALF	XGBoost	HistGBDT	GBDT	RandomForest	FT Transformer	Resnet	SAINT	MLP
default-credit-card	5.01E-03	6.30E-03	6.59E-03	7.43E-03	4.31E-03	3.98E-03	1.08E-02	5.69E-03	5.76E-03
eye_movements	9.21E-03	3.57E-03	7.36E-03	4.09E-03	5.22E-03	1.29E-02	6.68E-03	7.08E-03	1.16E-02
Mercedes	1.59E-02	8.41E-01	8.46E-01	8.42E-01	8.20E-01	8.35E-01	8.38E-01	8.71E-01	7.91E-01
topo_2_1	2.32E-02	4.21E-04	4.19E-04	4.42E-04	4.75E-04	4.67E-04	4.99E-04	5.35E-04	4.23E-04
Bioresponse	2.06E-02	1.74E-02	-	1.26E-02	1.32E-02	1.56E-02	1.00E-02	1.53E-02	1.32E-02
heloc	3.13E-03	1.06E-02	-	8.31E-03	1.31E-02	1.42E-02	1.26E-02	9.08E-03	1.02E-02
pol	1.01E-03	1.24E-03	-	2.34E-03	1.98E-03	2.36E-03	6.41E-03	3.91E-03	5.42E-03
Ailerons	1.12E-03	4.03E-06	4.58E-06	5.12E-06	-	1.14E-05	1.14E-05	2.54E-05	1.86E-06
cpu_act	2.75E-04	6.73E-02	2.13E-01	3.96E-02	-	2.56E-02	2.50E-02	6.83E-02	9.01E-02
yprop_4_1	2.95E-02	4.75E-04	-	5.40E-04	4.79E-04	3.96E-04	5.26E-04	4.37E-04	3.89E-04

Table 5: Test scores on TabSurvey(Borisov et al. 2022). For classification Accuracy and for regression Mean Squared Error score is reported. The best performing model is highlighted in bold and Standard deviation is reported as a \pm range.

Method	Adult	HIGGS	Covertype	Cal. Housing ¹
	Acc \uparrow	Acc \uparrow	Acc \uparrow	MSE \downarrow
XGBoost	87.3	77.6	97.3	0.206 \pm 0.005
CatBoost	87.2	77.5	96.4	0.196 \pm 0.004
GANDALF	86.7	76.9	97.7	0.16\pm0.006
LightGBM	87.4	77.1	93.5	0.195 \pm 0.005
SAINT	86.1	79.8	96.3	0.226 \pm 0.004
DeepFM	86.1	76.9	-	0.260 \pm 0.006
Net-DNF	85.7	76.6	94.2	-
NODE	85.6	76.9	89.9	0.276 \pm 0.005
TabNet	85.4	76.5	93.1	0.346 \pm 0.007
MLP	84.8	77.1	91.0	0.263 \pm 0.008
VIME	84.8	76.9	90.9	0.275 \pm 0.007
STG	85.4	73.9	81.8	0.285 \pm 0.006
Random Forest	86.1	71.9	78.1	0.272 \pm 0.006
Model Trees	85.0	69.8	-	0.385 \pm 0.019
Decision Tree	85.3	71.3	79.1	0.404 \pm 0.007
TabTransformer	85.2	73.8	76.5	0.451 \pm 0.014
DeepGBM	84.6	74.5	-	0.856 \pm 0.065
RLN	81.0	71.8	77.2	0.348 \pm 0.013
KNN	83.2	62.3	70.2	0.421 \pm 0.009
Linear Model	82.5	64.1	72.4	0.528 \pm 0.008
NAM	83.4	53.9	-	0.725 \pm 0.022

¹We binned Latitude and Longitude features and considered as Categorical Feature

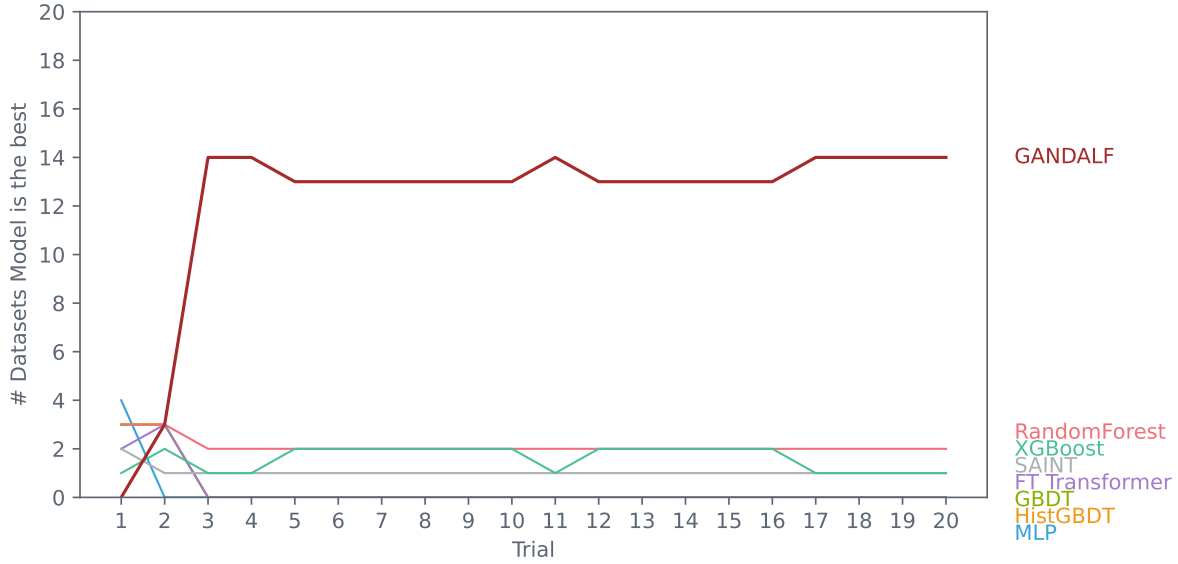


Figure 6: Hyperparameter Tuning Scenarios: If the random iterations were only N trials, how many datasets do a model become the best. We can see that GANDALF quickly takes the lead in 13 of 18 datasets in 5 trials (which is still in the random exploration stage of the hyperparameter tuning).

Table 6: Tuned Hyperparameters for each dataset in Tabular Benchmark (Grinsztajn, Oyallon, and Varoquaux 2022).

Dataset	GFLU Stages	Init Sparsity	GFLU Dropout	Learning Rate	Weight Decay
default-credit-card	2	0.870769	0.021064	0.001	0.001
heloc	13	0.291414	0.072046	0.001	0.0001
eye_movements	2	0.802989	0.011162	0.001	0.001
Higgs	10	0.717149	0.087058	0.001	1e-05
pol	3	0.181439	0.103777	0.001	1e-07
albert	18	0.007152	0.014137	0.001	1e-07
road-safety	19	0.001146	0.063497	0.001	1e-05
MiniBooNE	14	0.115137	0.002363	0.001	0.001
covertype	7	0.067178	0.056627	0.001	0.0001
jannis	2	0.309363	0.023717	0.001	1e-06
Bioresponse	2	0.103818	0.000808	0.0001	1e-05
cpu_act	21	0.529018	0.000493	0.001	1e-07
Ailerons	2	0.880892	0.003350	0.001	1e-07
yprop_4_1	9	0.193272	0.006030	0.001	1e-05
superconduct	21	0.151234	0.000635	0.001	1e-05
Allstate	27	0.609144	0.100092	0.0001	1e-05
topo_2_1	14	0.817548	0.057329	0.001	0.0001
Mercedes	30	0.031092	0.003284	0.0001	0.0001

Table 7: Tuned Hyperparameters for each dataset in TabSurvey (Borisov et al. 2022).

Dataset	GFLU Stages	Init Sparsity	GFLU Dropout	Learning Rate	Weight Decay
adult-income	20	0.242888	0.051258	0.001	0.001
Higgs	19	0.030949	0.085262	0.001	1e-05
covertype	18	0.36086	0.00226	0.001	0.0001
california-housing	14	0.121434	0.012372	0.001	1e-07

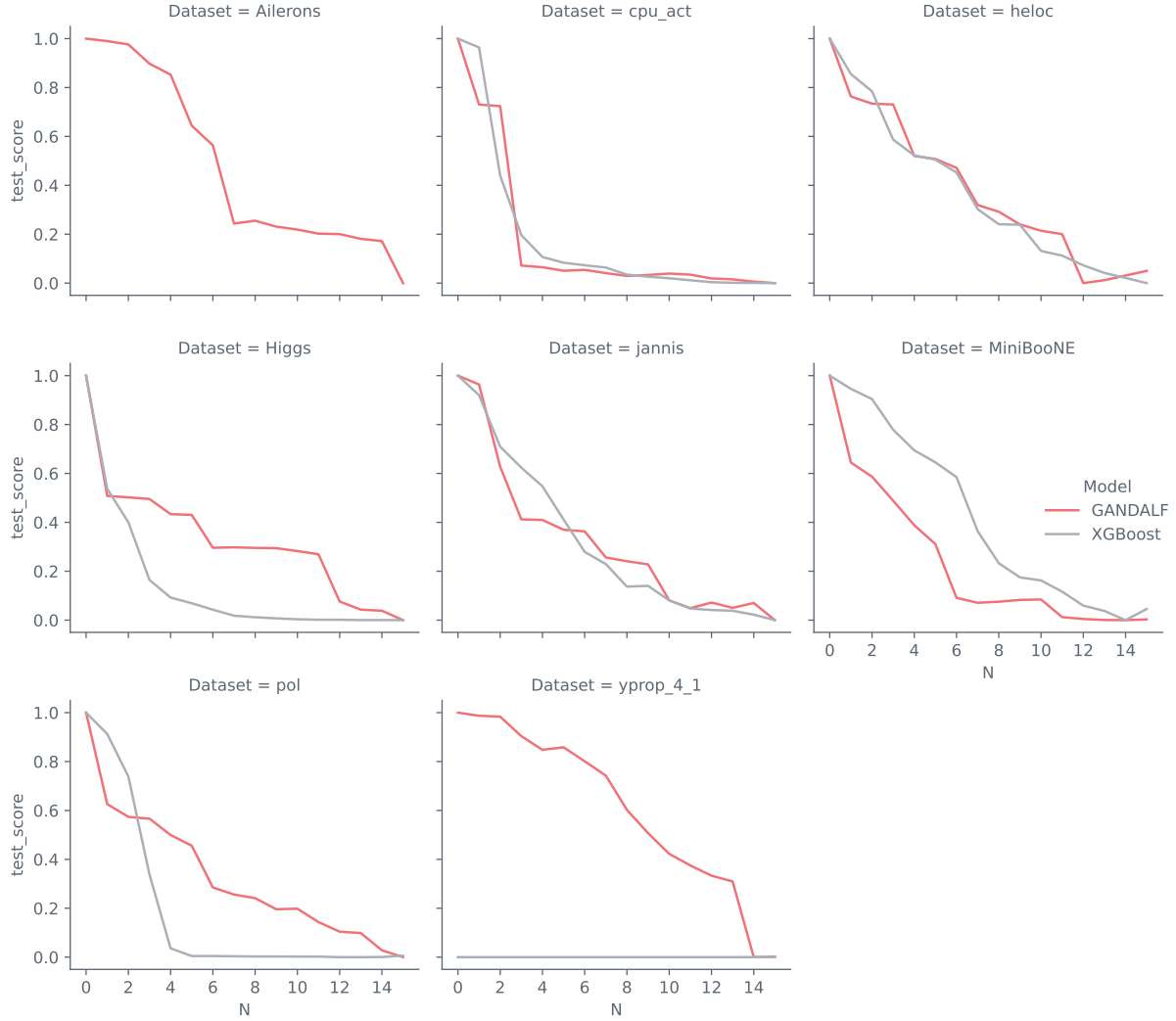


Figure 7: Feature Ablation (MoRF): GANDALF vs XGBoost for all datasets. We can see that the Test Scores drop drastically as we take out most relevant features, comparable to the XGBoost Feature importance.

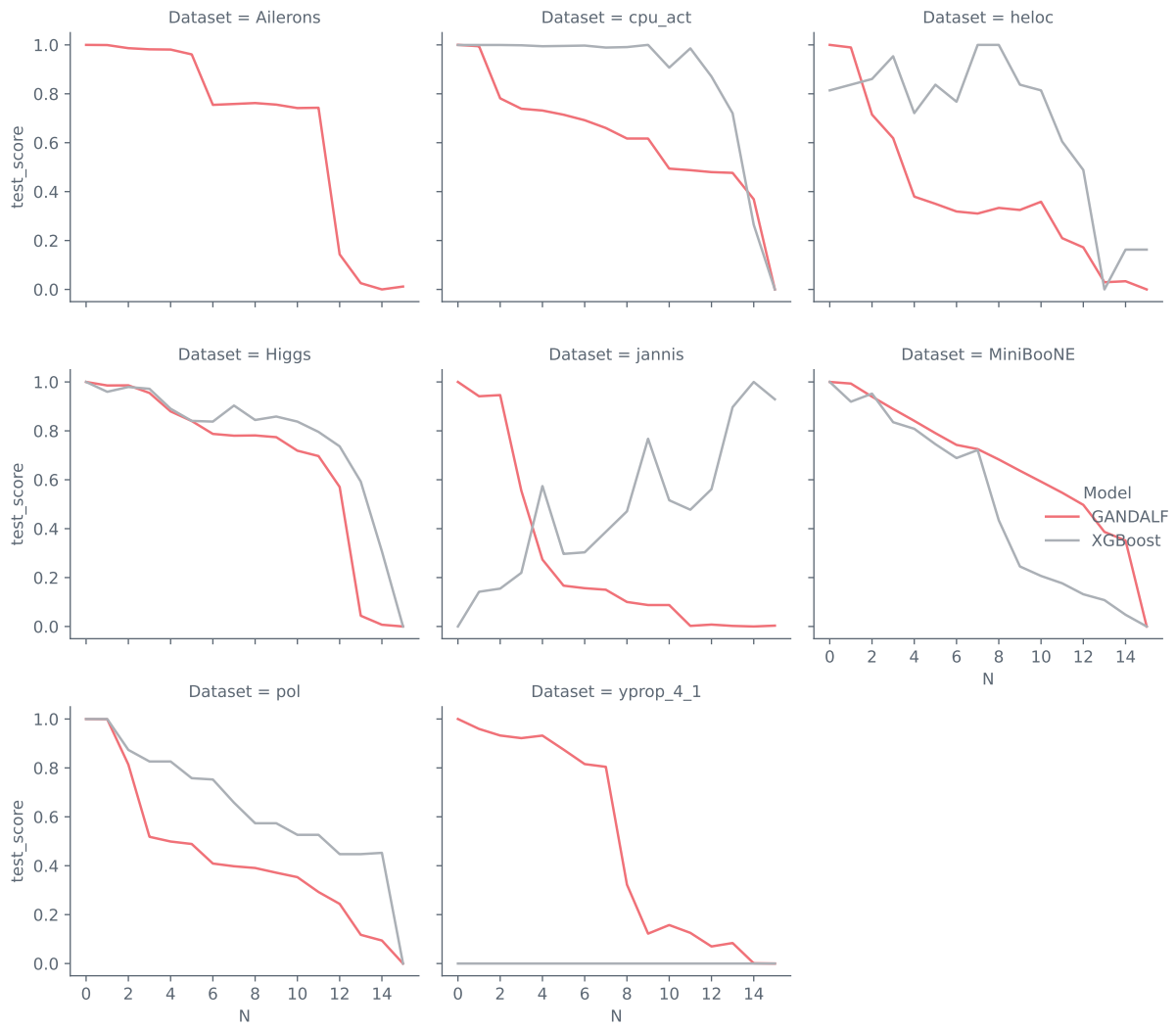


Figure 8: Feature Ablation (LeRF): GANDALF vs XGBoost for all datasets. We can see that the Test Scores do not drop as drastically as in MoRF as we take out least relevant features. *yprop_4_1* is a hard dataset and XGBoost test scores were too low to make an appearance in the chart.